CHEMISTRY
A EUROPEAN JOURNAL

ChemPubSoc
Europe

DOI: 10.1002/chem.201302018

Exploring the Effect of Bioisosteric Replacement of Carboxamide by a Sulfonamide Moiety on *N*-Glycosidic Torsions and Molecular Assembly: Synthesis and X-ray Crystallographic Investigation of *N*-(β-D-Glycosyl)sulfonamides as *N*-Glycoprotein Linkage Region Analogues

Amrita Srivastava,*[a] Babu Varghese,[b] and Duraikkannu Loganathan[a]

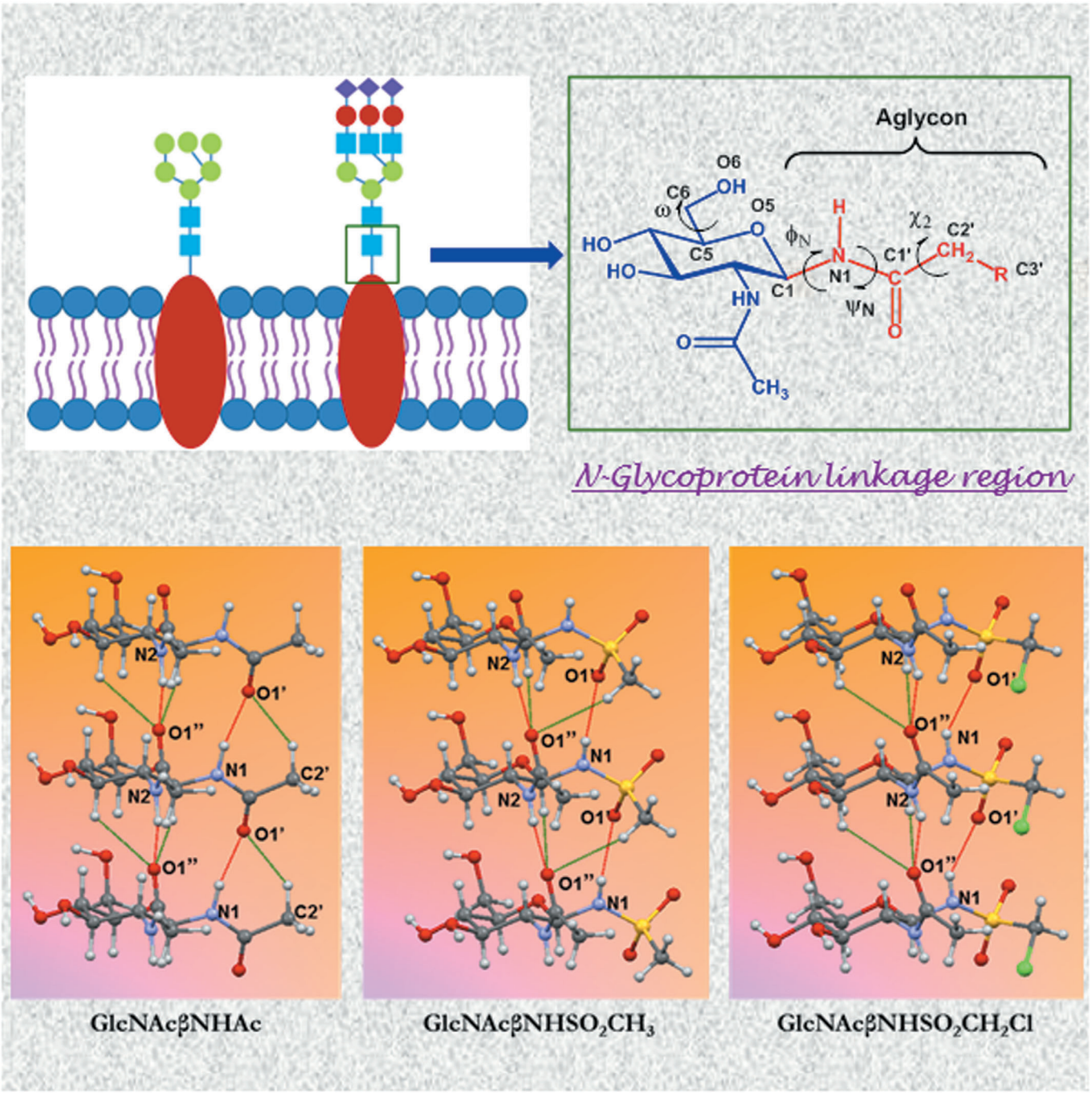

Abstract: *N*-Glycoprotein linkage region constituents, 2-acetamido-2-deoxy-β-D-glucopyranose (GlcNAc) and asparagine (Asn) are conserved among all the eukaryotes. To gain a better understanding for nature's choice of GlcNAcβAsn as linkage region constituents and inter- and intramolecular carbohydrate–protein interactions, a detailed systemic structural study of the linkage region conformation is essential. Earlier crystallographic studies of several *N*-(β-glycopyranosyl)alkanamides showed that *N*-glycosidic torsion, ϕ_N, is influenced to a larger extent by structural variation in the sugar part than that of the aglycon moiety. To explore the effect of the bioisosteric replacement of a carboxamide group by a sulfonamide moiety on the *N*-glycosidic torsions as well as on molecular assembly, several glycosyl methanesulfonamides and glycosyl chloromethanesulfonamides were synthesized as analogues of the *N*-glycoprotein linkage region, and crystal structures of seven of these compounds have been solved. A comparative analysis of this series of crystal structures as well as with those of the corresponding alkanamido derivatives revealed that *N*-glycosidic torsion, ϕ_N, does not alter significantly. Methanesulfonamido and chloromethanesulfonamido derivatives of GlcNAc display a different aglycon conformation compared to other sulfonamido analogues. This may be due to the cumulative effect of the direct hydrogen bonding between N1 and O1′ and C–H···O interactions of the aglycon chain, revealing the uniqueness of the GlcNAc as the linkage sugar.

Keywords: C–H···O interactions · *N*-glycoproteins · proteins · sulfonamides · X-ray diffraction

Introduction

Glycosylation is the most frequent, highly diverse post-translational covalent protein modification found in nature, occurring across all kingdoms of life.[1] Carbohydrate components of glycoproteins play important roles in many biological processes such as protein folding, inflammation, and bacterial and viral infection.[2,3] The GlcNAcβAsn linkage is conserved in *N*-glycoproteins of all eukaryotes (Figure 1).

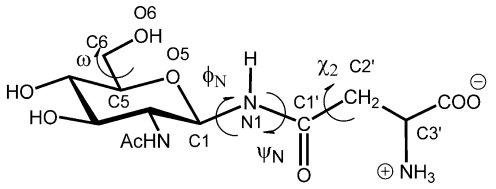

Figure 1. Schematic representation of the linkage region (GlcNAcβAsn) of the *N*-glycoproteins with the depiction of the torsion angles, ω = O5-C5-C6-O6, ϕ_N = O5-C1-N1-C1′, ψ_N = C1-N1-C1′-C2' and χ_2 = N1-C1′-C2′-C3′.

Elucidation of the conformation of the linkage region is of fundamental importance as the dynamics of the GlcNAc-Asn linkage can significantly influence the presentation of the glycan chains on the cell/protein surface. Understanding the structure–function correlations of the protein-linked glycans is certainly a challenging problem in glycobiology due to their structural complexity, micro-heterogeneity, flexibility, and non-availability in sufficient amounts. In this regard, use of *N*-glycoprotein linkage region models and analogues is a worthwhile approach which provides the finer details of atomic architecture and molecular recognition and also helps in understanding the effect of structural variation on the conformation of the linkage region.

A major program of our laboratory is focused on the synthesis, crystallography, and ab initio calculations of the *N*-glycoprotein linkage region models and analogues.[4–11] A systematic investigation pertaining to the effect of structural variation in the linkage region sugar and its aglycon moiety, among several *N*-(β-glycopyranosyl)alkanamido derivatives, on the *N*-glycosidic torsion, ϕ_N (O5-C1-N1-C1′) revealed that ϕ_N (Figure 1) is influenced to a larger extent by the structural variation in the sugar part than that of the aglycon moiety.[4] X-ray crystallographic analysis and ab initio calculations on the *N*-(β-D-glycopyranosyl)alkanamides showed that the *N*-acetyl group at C2 controls the side chain torsion angle χ_2 (N1-C1′-C2′-C3′) at the linkage region and helps in establishing the extended aglycon conformation.[7] Further studies on the various glycosyl alkanamides illustrated the influence of the substituent at C2 and C5 as well as environmental factors particularly inter- and intramolecular interactions involving hydrogen bonds and the weak C–H···O contacts on the energy preference of the ϕ_N torsion angle.[8] The critical role of C2-NHAc was also confirmed by the study of C3-NHAc analogues, which showed the *gauche* conformation of the amido aglycon moiety.[10] A comprehensive analysis of both the regular hydrogen bonds and the weak interactions involving C–H···O hydrogen bonds present in the crystal structures of *N*-glycoprotein models and analogues revealed a cooperative antiparallel network of bifurcated hydrogen bonds consisting of N–H···O and C–H···O interactions seen uniquely for the models, GlcNAcβAsn and GlcNAcβNHAc, and not for any analogue including the propionamide derivative, GlcNAcβNHPr. Such bifurcated

[a] Dr. A. Srivastava, Dr. D. Loganathan[+]
Department of Chemistry
Indian Institute of Technology Madras, Chennai - 600036 (India)
Fax: (+91) 44-22574202
E-mail: amrisriv9@gmail.com
[b] Dr. B. Varghese
Sophisticated Analytical Instrumentation Facility
Indian Institute of Technology Madras, Chennai - 600036 (India)
[+] Deceased on February 9, 2013.

Supporting information for this article is available on the WWW under http://dx.doi.org/10.1002/chem.201302018.

hydrogen bonds between the core glycan and protein could stabilize the linkage region conformation.[6,9]

To understand the effect of the bioisosteric replacement of a carboxamide with a sulfonamide moiety on the *N*-glycosidic torsion, ϕ_N and molecular assembly, several glycosyl methanesulfonamides and glycosyl chloromethanesulfonamides, which are very interesting glycosylasparagine analogues, have been designed and synthesized in the present work. Owing to its more acidic nature, introduction of a sulfonamide group increases the polarity and hydrogen-bond donor properties of a molecule. Moreover, due to the enormous stability towards enzymatic degradation and the structural similarity of the sulfonamido bond with the tetrahedral transition state involved in the enzymatic hydrolysis of an amide bond, these molecules can be used as enzyme inhibitors. Several glycosyl sulfonamides are known to be good inhibitors of carbonic anhydrases[12] and hepatocellular carcinoma cell lines.[13] Among all the glycosyl sulfonamides synthesized, X-ray crystal structures of seven (Figure 2) of these compounds have been solved. The molecular conformation and packing of these compounds were compared with this series as well as with the corresponding alkanamido derivatives. Glycosyl chloromethanesulfonamides were studied to examine the influence of chlorine, an electronegative substituent and potential hydrogen bond acceptor, on the molecular assembly.

Results and Discussion

Glycosyl sulfonamides can be synthesized from the glycosyl amines[14,15] or from per-*O*-acetylated sugars.[16] In the present work, acetylated glycosyl azides[17] were chosen as starting material. The fully acetylated β-D-glycosyl azides (**1**–**8**) were obtained by the displacement of their corresponding α-chlorides[18] with NaN_3 in aqueous acetone at room temperature.[19]

Synthesis and characterization

Synthesis of *N*-(β-D-glycosyl)methanesulfonamides: Per-*O*-acetylated β-D-glycosylamines were prepared by the reduction of per-*O*-acetylated β-D-glycosyl azides (**1**–**8**) using Pd/C and hydrogen in dry CH_2Cl_2. Reaction of these glycosyl amines with methanesulfonyl chloride in the presence of triethylamine afforded the per-*O*-acetylated *N*-(β-D-glycosyl)methanesulfonamides (**9**–**16**) in moderate to good yield with complete β-stereoselectivity (Scheme 1, Table 1). All

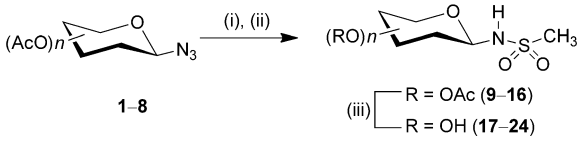

Scheme 1. Synthesis of *N*-(β-D-glycosyl)methanesulfonamides (**17**–**24**). Reagents and conditions: i) Pd/C, H_2, dry CH_2Cl_2, RT; ii) CH_3SO_2Cl, Et_3N, 0 °C–RT, ca. 8 h; iii) $Ba(OMe)_2$, dry MeOH, 0 °C–RT, 12 h.

the fully acetylated glycosyl methanesulfonamides (**9**–**16**) were taken up for de-*O*-acetylation using $Ba(OMe)_2$/MeOH at 0 °C. In all cases, deprotection was achieved in fairly good yield (Scheme 1, Table 1). All the products were characterized based on physical and spectral data. The ^1H NMR spectrum of the products displayed the anomeric proton signal around $\delta = 4.47$–4.95 ppm with a coupling constant of $J = 8.8$–9.6 Hz indicating the β-linkage.

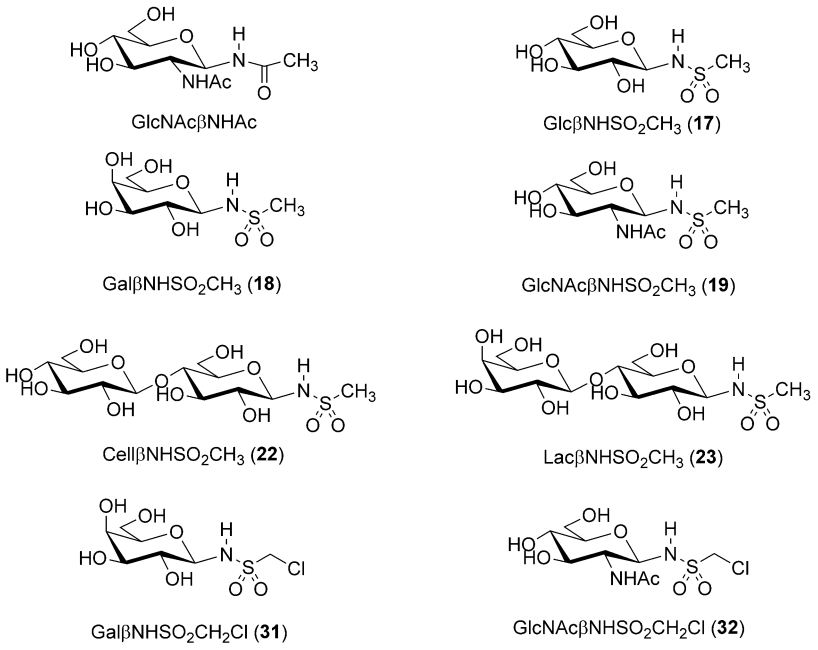

Figure 2. Structures of the model GlcNAcβNHAc and the sulfonamido analogues studied.

Synthesis of *N*-(β-D-glycopyranosyl)chloromethanesulfonamides: 2,3,4,6-Tetra-*O*-acetyl-β-D-glucopyranosylamine was allowed to react with chloromethanesulfonyl chloride under the same reaction conditions as used for the synthesis of fully acetylated glycosyl methanesulfonamides (**9**–**16**), which resulted in only 30% yield of the expected product. To improve the yield, the reaction was performed with different bases (*N*,*N*-diisopropylethylamine (DIEA), 4-dimethylaminopyridine (DMAP), and pyridine) and pyridine was found to be the best among all the bases chosen for the reaction. The maximum yield was obtained when pyridine was

Table 1. The *N*-(β-D-glycosyl)methanesulfonamides synthesized.

No.	Per-*O*-acetylated glycosyl azide	Per-*O*-acetylated Product	Yield [%]	De-*O*-acetylated Product	Yield [%]
1	GlcβN_3 (**1**)	**9**	70	**17**	95
2	GalβN_3 (**2**)	**10**	76	**18**	98
3	GlcNAcβN_3 (**3**)	**11**	70	**19**	93
4	ManβN_3 (**4**)	**12**	80	**20**	85
5	XylβN_3 (**5**)	**13**	50	**21**	90
6	CellβN_3 (**6**)	**14**	62	**22**	97
7	LacβN_3 (**7**)	**15**	53	**23**	90
8	MaltβN_3 (**8**)	**16**	30	**24**	80

used as a solvent. Per-*O*-acetylated β-D-glycosylamines were dried, dissolved in anhydrous pyridine and treated with chloromethanesulfonyl chloride at 0°C to afford the per-*O*-acetylated *N*-(β-D-glycopyranosyl)chloromethanesulfonamides (**25**–**29**) (Scheme 2, Table 2). All the fully acetylated glycosyl chloromethanesulfonamides (**25**–**29**) were de-*O*-acetylated by using NaOMe/MeOH at 0°C in very good yield (Scheme 2). All the products were characterized based

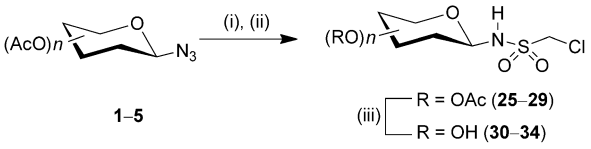

Scheme 2. Synthesis of *N*-(β-D-glycopyranosyl)chloromethanesulfonamides (**30**–**34**). Reagents and conditions: i) Pd/C, H_2, dry CH_2Cl_2, RT; ii) $ClCH_2SO_2Cl$, pyridine, 0°C–RT, ca. 3 h; iii) NaOMe, dry MeOH, 0°C–RT, 12 h.

Table 2. The *N*-(β-D-glycopyranosyl)chloromethanesulfonamides synthesized.

No.	Per-*O*-acetylated glycosyl azide	Per-*O*-acetylated Product	Yield [%]	De-*O*-acetylated Product	Yield [%]
1	GlcβN_3 (**1**)	**25**	75	**30**	85
2	GalβN_3 (**2**)	**26**	73	**31**	96
3	GlcNAcβN_3 (**3**)	**27**	70	**32**	90
4	ManβN_3 (**4**)	**28**	76	**33**	75
5	XylβN_3 (**5**)	**29**	60	**34**	90

on physical and spectral methods including ^1H and ^{13}C NMR spectroscopy. The ^1H NMR spectra of the products displayed the anomeric proton signal around $\delta = 4.50$–4.90 ppm with a coupling constant of $J = 8.8$–9.6 Hz indicating the β-linkage.

X-ray crystallographic investigation

Structure description: Among all the thirteen glycosyl sulfonamides synthesized, crystal structures of seven of them (**17**–**19**, **22**, **23**, **31**, and **32**) have been solved. The single crystals of all the free sulfonamides were obtained from aqueous methanol by using the slow evaporation method. The ORTEP representations of their solved structures with atom numbering are shown in Figure 3. All the *N*-(β-D-glycosyl)-methanesulfonamides (**17**, **19**, **22**, and **23**) crystallized in the monoclinic crystal system with a $P2_1$ space group except for *N*-(β-D-galactopyranosyl)methanesulfonamide (**18**), which crystallized in the *C*2 space group. Galβ$NHSO_2CH_3$ (**18**), GlcNAcβ$NHSO_2CH_3$ (**19**), and Lacβ$NHSO_2CH_3$ (**23**) crystallized as monohydrates, whereas Glcβ$NHSO_2CH_3$ (**17**) and Cellβ$NHSO_2CH_3$ (**22**) turned out to be anhydrous crystalline solids. The two *N*-(β-D-glycopyranosyl)chloromethanesulfonamides (**31** and **32**) crystallized in the orthorhombic crystal system with a $P2_12_12_1$ space group. Galβ$NHSO_2CH_2Cl$ (**31**) crystallized in anhydrous form, whereas GlcNAcβ$NHSO_2CH_2Cl$ (**32**) crystallized as a monohydrate. The β anomeric configuration of compounds **17**–**19**, **22**, **23**, **31**, and **32** was evident from the ORTEP representation (Figure 3). All atoms of the reducing end residue of the disaccharides are numbered with a suffix A, whereas those of non-reducing end residue are numbered with a suffix B. The pyranose ring adopts a $^4C_1$ conformation in all the seven crystals. Lists of selected bond lengths and bond angles are provided in Table 3 and Table 4, respectively. Geometrical parameters for all the crystals are compared with the series as well as with those already reported for alkanamido derivatives. Two different conformers were present in the asymmetric unit of Cellβ$NHSO_2CH_3$ (**22**) labeled as A and B.

The C–C bond lengths in all these compounds are close to 1.54 Å, which is observed in most sugar derivatives.[20]

Table 3. Selected bond lengths [Å] in compounds **17**–**19**, **22**, **23**, **31**, and **32**.

Parameter	Glcβ$NHSO_2CH_3$ (**17**)	Galβ$NHSO_2CH_3$·H_2O (**18**)	GlcNAcβ$NHSO_2CH_3$·H_2O (**19**)	Cellβ$NHSO_2CH_3$ (**22A**)	Cellβ$NHSO_2CH_3$ (**22B**)	Lacβ$NHSO_2CH_3$·H_2O (**23**)	Galβ$NHSO_2CH_2Cl$ (**31**)	GlcNAcβ$NHSO_2CH_2Cl$·H_2O (**32**)
C1–O5	1.424(3)	1.420(2)	1.421(2)	1.426(3) 1.431(3)	1.433(3) 1.425(3)	1.424(3) 1.427(3)	1.421(3)	1.437(4)
C5–O5	1.431(3)	1.432(2)	1.429(3)	1.436(3) 1.440(3)	1.432(3) 1.440(3)	1.435(3) 1.437(3)	1.434(2)	1.413(4)
C1–N1	1.431(3)	1.442(2)	1.428(2)	1.449(3)	1.438(3)	1.440(3)	1.431(3)	1.410(5)
S1–N1	1.635(2)	1.621(1)	1.611(2)	1.635(2)	1.626(2)	1.620(2)	1.603(2)	1.605(4)
S1–O1′	1.428(2)	1.434(1)	1.430(2)	1.439(2)	1.410(3)	1.413(2)	1.425(2)	1.397(3)
S1–O2′	1.445(2)	1.427(2)	1.424(2)	1.425(2)	1.439(3)	1.425(2)	1.426(2)	1.435(4)
S1–C2′	1.753(3)	1.752(3)	1.740(3)	1.755(3)	1.742(3)	1.738(3)	1.784(2)	1.763(5)
C2′–Cl	–	–	–	–	–	–	1.751(2)	1.747(5)
C1–C2	1.529(3)	1.531(2)	1.528(3)	1.541(3) 1.506(3)	1.530(3) 1.516(3)	1.517(3) 1.512(3)	1.521(3)	1.540(5)

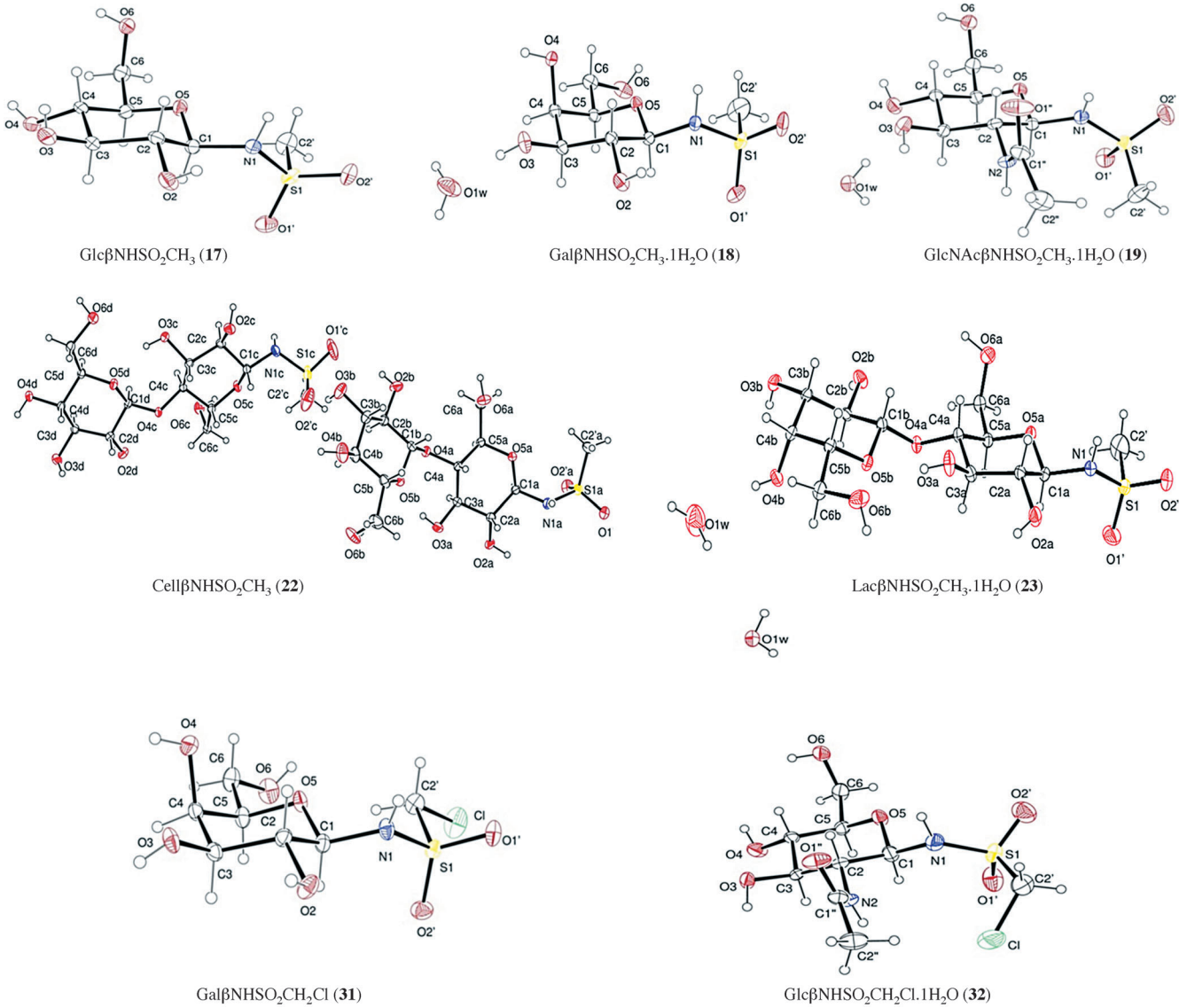

Figure 3. ORTEP representations (probability 30%) of the crystal structures of compounds **17**–**19**, **22**, **23**, **31**, and **32**.

Table 4. Selected bond angles [°] in compounds **17**–**19**, **22**, **23**, **31** and **32**.

Parameter	GlcβNH SO_2CH_3 (**17**)	GalβNH SO_2CH_3·H_2O (**18**)	GlcNAcβNH SO_2CH_3·H_2O (**19**)	CellβNH SO_2CH_3 (**22A**)	CellβNH SO_2CH_3 (**22B**)	LacβNH SO_2CH_3·H_2O (**23**)	GalβNH SO_2CH_2Cl (**31**)	GlcNAcβNH SO_2CH_2Cl·H_2O (**32**)
O5-C1-N1	109.1(2)	107.5(1)	108.4(2)	107.8(2)	107.9(2)	109.0(2)	108.6(2)	108.1(3)
C2-C1-N1	111.5(2)	109.6(1)	112.2(2)	108.3(2)	110.7(2)	108.9(2)	111.5(2)	112.6(3)
N1-S1-O1′	108.0(1)	107.74(8)	108.0(1)	105.8(1)	106.6(2)	106.8(1)	106.9(1)	111.2(2)
N1-S1-O2′	105.0(1)	105.44(8)	107.3(1)	107.2(1)	107.5(1)	105.7(1)	109.1(1)	108.8(2)
O1′-S1-O2′	118.5(1)	118.34(9)	119.5(1)	118.8(1)	117.4(2)	119.0(1)	118.5(1)	119.2(2)
S1-C2′-Cl	–	–	–	–	–	–	109.5(1)	113.0(2)
C4-C5-C6	112.6(2)	112.9(1)	114.7(2)	116.1(2) 114.9(2)	113.7(2) 114.6(2)	114.2(2) 113.3(2)	113.8(2)	114.2(3)
O5-C5-C6	106.9(2)	106.7(1)	107.5(2)	109.1(2) 105.8(2)	107.5(2) 106.4(2)	107.7(2) 106.3(2)	107.0(2)	107.2(3)
C5-C6-O6	111.6(2)	111.2(1)	113.6(2)	109.9(2) 113.2(3)	111.6(2) 108.9(2)	110.6(2) 109.5(2)	111.6(2)	112.8(3)
C5-O5-C1	112.1(2)	112.8(1)	112.1(2)	112.3(2) 113.6(2)	110.8(2) 112.1(2)	112.1(2) 113.1(2)	111.8(2)	112.3(3)
C1-N1-S1	118.1(2)	120.0(1)	121.7(1)	120.1(2)	117.6(2)	120.8(2)	121.0(2)	123.1(3)
C1-N1-H1N	116(2)	114(1)	119.1	112(2)	115(2)	114(2)	121(2)	107(3)
S1-N1-H1N	110(2)	108(1)	119.1	110(2)	110(2)	111(2)	116(2)	125(3)

Among the C–O bond lengths, The C5–O5 bond lengths are found to be longer than the C1–O5 bond lengths for compounds GlcβNHSO$_2$CH$_3$ (**17**), GalβNHSO$_2$CH$_3$ (**18**), GlcNAcβNHSO$_2$CH$_3$ (**19**), LacβNHSO$_2$CH$_3$ (**23**), and GalβNHSO$_2$CH$_2$Cl (**31**), as seen in most of the β-1-*N*-alkanamido sugar derivatives, whereas the reverse was true for GlcNAcβNHSO$_2$CH$_2$Cl (**32**). In the case of conformer A of CellβNHSO$_2$CH$_3$ (**22**), the C5–O5 bond is longer than the C1–O5 bond (in both the non-reducing end residue and reducing end residue) but both the bond lengths (C1–O5 and C5–O5) were equal in the case of the reducing end residue of conformer B. The C–N bond lengths (C1–N1) for all the compounds **17**–**19**, **22**, **23**, **31**, and **32** were 1.41–1.44 Å in good agreement with the value of 1.44 Å observed for GlcNAcβAsn.[21] The S–N bond lengths (S1–N1) for all the compounds **17**–**19**, **22**, **23**, **31**, and **32** were in the range of 1.60–1.64 Å, which is less than the normal length of a single bond (1.73 Å). This can be explained by the donor–acceptor interaction of the unshared electron pair in the amido-group nitrogen atom with the 3d orbitals of the sulfur atom. The length of the S–O bond agrees with the average value found in other sulfonamides reported in the literature. All the angles involving carbon are close to the tetrahedral value of 109.5° (Table 4). The *N*-glycosidic valence angle, O5-C1-N1, is smaller than that of C2-C1-N1 for compounds **17**–**19**, **22**, **31**, and **32** except for LacβNHSO$_2$CH$_3$ (**23**). The exocyclic bond angles, namely C4-C5-C6 and O5-C5-C6 have a mean value of 114.1° and 107.1°, respectively, with the latter being consistently smaller than the former. Due to the presence of a lone pair of electrons, the valence angle at the ring oxygen atom, namely C5-O5-C1 deviates from the tetrahedral by about 1–5°. This variation is seen in all the compounds **17**–**19**, **22**, **23**, **31**, and **32**. The valance angles at the S atom are quite different from the tetrahedral angle; < O-S-O = 117–119°, giving the sulfonamido group as a distorted tetrahedral geometry.

Molecular conformation: The molecular conformation of the compounds **17**–**19**, **22**, **23**, **31**, and **32** is defined by the torsion angles, ω, ω′, ϕ_0, ψ_0, ϕ_N, ψ_N, and χ_2 (Figure 4, Table 5). The hydroxymethyl group adopts a *gg* conformation in GlcβNHSO$_2$CH$_3$ (**17**), GlcNAcβNHSO$_2$CH$_3$ (**19**), and GlcNAcβNHSO$_2$CH$_2$Cl (**32**), as evident from the values of the torsion angles, O5-C5-C6-O6 (ω, ca. −60°) and C4-C5-C6-O6 (ω′, ca. 60°). For the compounds GalβNHSO$_2$CH$_3$ (**18**) and GalβNHSO$_2$CH$_2$Cl (**31**), in which the C4-OH group is in an axial position, the hydroxymethyl group adopts a *gt* conformation with the torsion angles, ω, close to 63° and ω' around −175°. In the case of CellβNHSO$_2$CH$_3$ (**22**), however, the two conformers A and B differ in the conformation of the hydroxymethyl group. The hydroxymethyl group in conformer A adopts a *gg* conformation in both the reducing end residue as well as the non-reducing

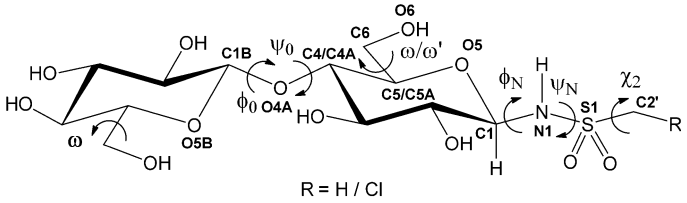

Figure 4. Depiction of the various torsion angles, ω = O5-C5-C6-O6, ω′ = C4-C5-C6-O6, ϕ_O = C4A-O4A-C1B-O5B, Ψ_O = C1B-O4A-C4A-C5A, ϕ_N = O5-C1-N1-S1, ψ_N = C1-N1-S1-C2′ and χ_2 = N1-S1-C2′-Cl.

Table 5. Selected torsion angles [°] of compounds **17**–**19**, **22**, **23**, **31**, **32**, and related compounds.

Compound	O5-C1-N1-C1′/S1 (ϕ_N)	C1-N1-C1′/S1-C2′ (ψ_N)	N1-C1′/S1-C2′-Cl (χ_2)	O5-C5-C6-O6 (ω)	C4-C5-C6-O6 (ω′)	C4A-O4A-C1B-O5B (φ_O)	C1B-O4A-C4A-C5A (ψ_O)	H1-C1-N1-N1H
GlcNAcβAsn·3H$_2$O[21]	−98.9	180.0	−172.2	−60.4	59.8	–	–	–
GlcNAcβNHAc·H$_2$O[32]	−89.8(1)	174.2(2)	–	−66.4(2)	55.4(2)	–	–	−161.9
GlcβNHAc[33]	−93.8(2)	−179.2(3)	–	−71.8(3)	50.1(4)	–	–	−154.8
GalβNHAc[4]	−105.2(3)	178.5(3)	–	60.5(3)	−177.1(2)	–	–	−171.0
ManβNHAc[4]	−114.5(2)	171.3(2)	–	−55.5(2)	67.0(2)	–	–	177.3
LacβNHAc[24]	−100.9(2)	175.1(2)	–	−59.3(2)[a] 58.3(3)[b]	62.4(3)[a] 179.0(2)[b]	−89.3(2)	−157.8(2)	−162.5(2)
GalβNHCOCH$_2$Cl[34]	−111.5(3)	176.6(3)	153.3(2)	61.7(3)	−175.8(2)	–	–	174.4
GlcNAcβNHCOCH$_2$Cl[7]	−91.7(6)	173.6(7)	173.0(6)	−53.7(7)	67.0(6)	–	–	164.7
GlcβNHSO$_2$CH$_3$ (**17**)	−85.5(2)	70.9(2)	–	−62.0(3)	60.7(3)	–	–	167(2)
GalβNHSO$_2$CH$_3$·H$_2$O (**18**)	−83.7(1)	69.4(2)	–	63.6(2)	−176.4(1)	–	–	166(1)
GlcNAcβNHSO$_2$CH$_3$·H$_2$O (**19**)	−97.0(2)	−94.8(2)	–	−66.7(2)	55.5(3)	–	–	−158.5(2)
CellβNHSO$_2$CH$_3$ (**22A**)	−81.7(2)	77.1(2)	–	−70.6(2)[a] −61.7(3)[b]	49.3(3)[a] 58.9(4)[b]	−80.9(2)	−124.5(2)	169(2)
CellβNHSO$_2$CH$_3$ (**22B**)	−76.6(2)	74.7(3)	–	−64.3(2)[a] 57.7(3)[b]	56.2(3)[a] 175.8(2)[b]	−86.9(2)	−144.0(2)	174(2)
LacβNHSO$_2$CH$_3$·H$_2$O (**23**)	−81.9(2)	70.6(2)	–	−57.0(2)[a] 61.3(2)[b]	63.5(2)[a] −177.4(2)[b]	−90.0(2)	−156.8(2)	175(2)
GalβNHSO$_2$CH$_2$Cl (**31**)	−76.2(2)	68.7(2)	−177.9(1)	63.1(3)	−174.9(2)	–	–	−156(2)
GlcNAcβNHSO$_2$CH$_2$Cl·H$_2$O (**32**)	−90.3(4)	−125.2(4)	67.1(3)	−68.6(4)	54.7(4)	–	–	−174(3)

[a] Reducing end residue. [b] Non-reducing end residue.

end residue as evident from the values of the torsion angles, ω (−70°) and ω' (49°) for the reducing end residue and ω (−62°) and ω' (59°) for the non-reducing end residue. The torsion angle values of −64° and 56° of conformer B for the reducing end residue and 57° and 176° for the non-reducing end residue reveal the *gg* conformation of the former and *gt* conformation of the later. The hydroxymethyl group in LacβNHSO$_2$CH$_3$ (**23**) adopts the *gg* conformation (ω, −57° and ω′, 63°) in the reducing end residue and the *gt* conformation (ω, 61° and ω′, −177°) in the non-reducing end residue. The *gt* conformation is also noted in many of the cellobiose derivatives.[22]

The inter glycosidic torsions angles ϕ_0 and ψ_0 of analogue **22A** are −80.9(2)° and −124.5(2)°, respectively, whereas for analogue **22B**, the values are −86.9(2)° and −144.0(2)°, respectively. These angles compare well with those reported for cellobiose related structures.[23] Torsion angle ϕ_0 and ψ_0 values for LacβNHSO$_2$CH$_3$ (**23**) are −90.0(2) and −156.8(2)°, respectively, which are comparable to the values of −89.3(2)° and −157.8(2)° observed for LacβNHAc.[24] For most of the compounds (**17**, **18**, **22**, **23** and **31**), values of torsion angle ψ_N were close to about 75° except for methanesulfonamido (**19**) and chloromethanesulfonamido (**32**) derivatives of GlcNAc. The values of torsion angle ψ_N for compounds **19** and **32** were −94.8(2)° and −125.2(4)°, respectively. The aglycon chain of methanesulfonamido (**19**) and chloromethanesulfonamido (**32**) derivatives of GlcNAc adopts a different aglycon conformation as evident from their torsion angle (ψ_N) values. The conformation about the C1−N1 bond is *anti* in all the compounds as evident from the values of the torsion angle H1-C1-N1-N1H, which is greater than 150°.

The *N*-glycosidic linkage torsion angle ϕ_N (O5-C1-N1-S1) values for GlcβNHSO$_2$CH$_3$ (**17**), GalβNHSO$_2$CH$_3$ (**18**), GlcNAcβNHSO$_2$CH$_3$ (**19**), conformer A of CellβNHSO$_2$CH$_3$ (**22**), LacβNHSO$_2$CH$_3$ (**23**), and GlcNAcβNHSO$_2$CH$_2$Cl (**32**) are close to the values reported for the model GlcNAcβNHAc (Table 5, Figure 5). In the case of conformer B of CellβNHSO$_2$CH$_3$ (**22**) and GalβNHSO$_2$CH$_2$Cl (**31**), the ϕ_N values are −76.6(2)° and −76.2(2)°, respectively, which deviates by a maximum of approximately 15° from the model compound, GlcNAcβNHAc. This indicates that *N*-glycosidic torsion, ϕ_N does not vary significantly by changing the linkage from a carboxamido group to a sulfonamido moiety. Variation in the torsion angle χ_2 (N1-S1-C2′-Cl) among GalβNHSO$_2$CH$_2$Cl (**31**) and GlcNAcβNHSO$_2$CH$_2$Cl (**32**) was also examined and the values are found to be −177.9(1)° and 67.1(3)°, respectively, in contrast to the value of 153.3(2)° reported for GalβNHCOCH$_2$Cl and of 173.0(6)° reported for GlcNAcβNHCOCH$_2$Cl. The near *anti* conformation about S1−C2′ bond exhibited by compound **31**, gets altered to a *gauche* conformation in the compound **32**. Such a large difference in χ_2 value is noteworthy. Earlier conformational calculations on sulfonamide-containing small molecules showed the energy difference among the two forms (*gauche* and *anti*) to be much less (ca. 0.7 KJ mol^{-1}). However, in the solid state, hydrogen bonding, C−H···O interactions and crystal packing forces might strongly influence the conformations adopted.[25]

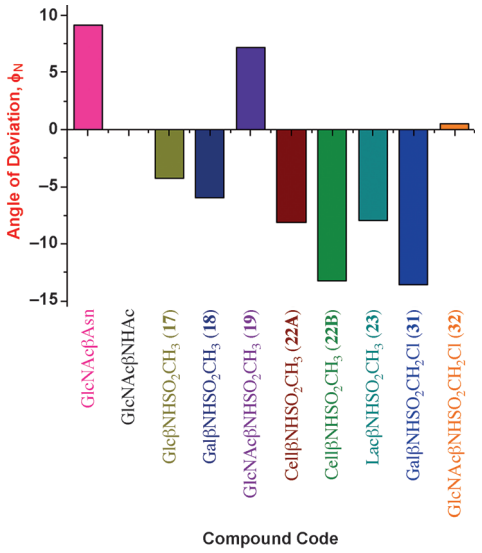

Figure 5. Graphical representation of the variation of ϕ_N values of *N*-(β-D-glycosyl)sulfonamides relative to that of GlcNAcβNHAc.

Molecular packing: The various hydrogen bonds present in the crystal structures of compounds **17**–**19**, **22**, **23**, **31**, and **32** were analyzed and their parameters are listed in Table 6 and 8. The molecular packing is stabilized by several N−H···O, O−H···O as well as C−H···O interactions occurring through finite and infinite chains of hydrogen bonds (Table 7).

Finite and infinite chain: In all the compounds (**17**–**19**, **22**, **23**, **31**, and **32**), N1 is connected to O1′ or O2′ through a finite chain of hydrogen bonds except for CellβNHSO$_2$CH$_3$ (**22**). In GlcβNHSO$_2$CH$_3$ (**17**), the finite chain begins with N1, passes through O4, O2, O6, O3 of symmetry-related molecules and ends at O2′. The Gal derivative GalβNHSO$_2$CH$_3$ (**18**) differs from Glc (**17**) in terms of the altered sequence of oxygen atoms of symmetry-related molecules. In GalβNHSO$_2$CH$_3$ (**18**), the finite chain starts with N1, passes through O3 and bifurcates at O1W into two finite chains. One chain ends at O1′ and another chain runs through O6, O2, and O4 and finally ends at O2′ (see Figure S1 in the Supporting Information). The characteristic feature of GlcNAc derivatives is the direct hydrogen bonding between N1 and O1′ accompanied by a similar one involving N2 and O1″ leading to double-pillared molecular packing along the crystallographic *a* axis. This feature is also found in GlcNAcβNHSO$_2$CH$_3$ (**19**) (Figure 6) and GlcNAcβNHSO$_2$CH$_2$Cl (**32**) (see Figure S2 in the Supporting Information). Similar to the packing in GlcNAcβNHAc, that in GlcNAcβNHSO$_2$CH$_3$ (**19**) is stabilized by two infinite chains of hydrogen bonds. The first one involves the water molecule (O1W), O3, and O6 atoms, and propagates along the *b* axis (Figure 7). In the second one, the water molecule acts as a donor as well as an acceptor to its neighboring O4

Table 6. Hydrogen bond parameters for compounds **17**–**19**, **22**, **23**, **31**, and **32**.

D–H···A	D–H [Å]	H–A [Å]	D–A [Å]	D–H···A [°]	Symmetry
Glcβ$NHSO_2CH_3$ (**17**)					
N1–H1N···O4	0.84(3)	1.98(3)	2.802(3)	165(2)	$x-1, y, z$
O4–H4O···O2	0.82	1.89	2.664(3)	156.6	$-x+1, y+1/2, -z+1$
O6–H6O···O3	0.82	1.95	2.759(3)	170.4	$-x+1, y+1/2, -z+1$
O3–3O···O2′	0.82	2.04	2.856(3)	172.4	$-x, y+1/2, -z+1$
O2–H2O···O6	0.82	1.99	2.801(2)	170.5	$-x, y-1/2, -z+1$
Galβ$NHSO_2CH_3{\cdot}H_2O$ (**18**)					
N1–H1N···O3	0.86(2)	2.05(2)	2.881(2)	162(2)	$-x+3/2, y-1/2, -z$
O4–H4O···O2′	0.82	1.96	2.758(2)	164.7	$x, y, z+1$
O1W–H2W···O1′	0.83(2)	2.10(2)	2.899(2)	162(3)	$x, y, z+1$
O6–H6O···O2	0.82	1.98	2.787(2)	168.2	$x, y-1, z$
O2–H2O···O4	0.82	1.96	2.780(1)	174.7	$-x+3/2, y+1/2, -z$
O1W–H1W···O6	0.80(2)	1.98(2)	2.772(2)	171(3)	$-x+2, y+1, -z+1$
O3–H3O···O1W	0.82	1.88	2.689(2)	170.8	–
GlcNAcβ$NHSO_2CH_3{\cdot}H_2O$ (**19**)					
N1–H1N···O1′	0.86	2.13	2.929(2)	154.0	$x+1, y, z$
N2–H2N···O1″	0.86	2.04	2.807(2)	148.3	$x-1, y, z$
O1W–H2W···O3	0.82(2)	1.96(2)	2.737(2)	159(3)	$x-1, y, z$
O3–H3O···O6	0.82	1.96	2.758(2)	163.3	$x, y+1, z$
O4–H4O···O1W	0.82	1.95	2.745(3)	163.3	$-x+1, y-1/2, -z$
O6–H6O···O1W	0.82	1.98	2.767(3)	159.6	$-x+1, y-1/2, -z$
O1W–H1W···O4	0.83(2)	1.90(2)	2.721(3)	170(3)	–
Cellβ$NHSO_2CH_3$ (**22**)					
N1A–H1NA···O2A	0.85(1)	2.20(1)	3.033(3)	168(3)	$-x+1, y+1/2, -z+2$
N1C–H1NC···O3B	0.85(1)	2.23(1)	3.065(4)	173(3)	$-x+2, y-1/2, -z+1$
O2A–H2OA···O2D	0.82	1.92	2.705(2)	160.4	$-x+1, y+1/2, -z+1$
O2C–H2OC···O4D	0.82	1.98	2.798(2)	171.6	$-x+2, y+1/2, -z$
O2D–H2OD···O6A	0.82	1.93	2.739(3)	169.2	$x, y-1, z-1$
O3D–H3OD···O1′A	0.82	2.08	2.899(3)	173.8	$-x+1, y-1/2, -z+1$
O4B–H4OB···O1′A	0.82	2.41	3.166(3)	153.3	$x, y, z-1$
O4D–H4OD···O6B	0.82	1.95	2.739(2)	160.2	$-x+1, y-1/2, -z$
O6A–H6OA···O3C	0.82	2.01	2.833(2)	175.0	$-x+2, y+1/2, -z+1$
O3C–H3OC···O5D	0.82	2.04	2.818(2)	157.1	x, y, z
O3A–H3OA···O5B	0.82	2.12	2.893(3)	157.9	x, y, z
O6B–H6OB···O4B	0.82	2.17	2.934(3)	154.8	$-x+1, y-1/2, -z+1$
O6C–H6OC···O1′C	0.82	1.89	2.712(3)	179.1	$-x+2, y-1/2, -z+1$
O6D–H6OD···O6C	0.82	1.96	2.735(3)	156.6	$-x+2, y+1/2, -z$
Lacβ$NHSO_2CH_3{\cdot}H_2O$ (**23**)					
N1–H1N···O1′	0.81(2)	2.05(2)	2.837(3)	162(3)	$x+1, y, z$
O3A–H3OA···O5B	0.82	2.03	2.763(2)	148.0	–
O3A–H3OA···O6B	0.82	2.44	3.079(3)	135.6	–
O2B–H2OB···O3A	0.82	1.97	2.769(2)	163.1	$x, y, z+1$
O3B–H3OB···O6B	0.82	1.95	2.757(3)	166.1	$x, y, z+1$
O6B–H6OB···O3B	0.82	1.93	2.749(2)	176.9	$x-1, y, z-1$
O6A–H6OA···O2A	0.82	2.01	2.823(2)	171.4	$x+1, y, z+1$
O2A–H2OA···O2B	0.82	1.95	2.727(2)	157.6	$x-1, y, z-1$
O1W–H1W···O2′	0.84(2)	1.99(2)	2.812(4)	166(4)	$-x+1, y-1/2, -z$
O1W–H2W···O6A	0.81(2)	2.50(5)	3.016(3)	123(5)	$-x+2, y-1/2, -z+1$
O4B–H4OB···O1W	0.82	1.99	2.802(3)	171.2	x, y, z
Galβ$NHSO_2CH_2Cl$ (**31**)					
N1–H1N···O3	0.82(1)	2.06(1)	2.857(2)	165(3)	$-x, y-1/2, -z+1/2$
O2–H2O···O1′	0.82	2.33	2.864(2)	122.8	$-x, y+1/2, -z+1/2$
O2–H2O···O2′	0.82	2.34	3.077(2)	150.8	$-x+1, y+1/2, -z+1/2$
O4–H4O···O1′	0.82	2.29	2.993(2)	144.8	$x, y+1, z$
O3–H3O···O2	0.82	1.92	2.745(2)	178.6	$-x+1, y+1/2, -z+1/2$
O6–H6O···O6	0.82	2.03	2.845(2)	170.6	$x-1/2, -y+1/2, -z+1$
GlcNAcβ$NHSO_2CH_2Cl{\cdot}H_2O$ (**32**)					
N1–H1N···O1′	0.87(2)	2.11(3)	2.898(5)	150(4)	$x+1, y, z$
N2–H2N···O1″	0.85(2)	2.06(3)	2.821(4)	149(4)	$x-1, y, z$
O4–H4O···O1W	0.82	1.94	2.737(4)	163.5	$-x+1, y-1/2, -z+1/2$
O6–H6O···O1W	0.82	1.98	2.760(4)	158.4	$-x+1, y-1/2, -z+1/2$
O1W–H2W···O3	0.82(2)	1.92(2)	2.713(4)	166(5)	$x, y+1, z$
O1W–H1W···O4	0.83(2)	1.88(2)	2.706(4)	175(5)	$x+1, y+1, z$
O3–H3O···O6	0.82	1.94	2.750(4)	168.8	$x, y-1, z$

atoms facilitating the formation of a homodromic hydrogen-bonded network (Figure 8). Thus, the water molecule is tetra-coordinated donating both the hydrogens to O3 and O4, while acting as an acceptor for O4 and O6 leading to the formation of claw-shaped hydrogen bonds (Figure 7).

In Cellβ$NHSO_2CH_3$ (**22**), one finite chain starts from N1A, passes through O2A, O2D, O6A, and O3C of symmetry-related molecules and ends at O5D. Another finite chain starts from O2C, running through O4D, O6B, O4B and finally ends at O1′A (see Figure S3 in the Supporting Information). O1′A acts as a double acceptor for O3D and O4B atoms (O3D–H3OD···O1′A···H4OB–O4B). O6C acts as a donor (O6C–H6OC···O1′C) as well as an acceptor atom (O6D–H6OD···O6C). Two direct hydrogen bonds are also present which lend further stabilization (N1C–H1NC···O3B and O3A–H3OA···O5B). Lacβ$NHSO_2CH_3$ (**23**) exhibits direct hydrogen bonding between N1 and O1′. Molecular packing of **23** is stabilized by one infinite and one finite chain of hydrogen bonds. The finite chain starts from O4B, passes through O1W, O6A, O2A, O2B, and O3A of symmetry-related molecules and ends at O5B. O3A acts as a bifurcated donor (O3A–H3OA···O5B and O3A–H3OA···O6B). The infinite chain involves O3B and O6B acting as donor and acceptor and runs along the *a* axis. This pattern is similar to that in Lacβ$NHAc.2H_2O$.[24] In addition, one direct hydrogen bond is also present (O1W–H1W···O2′). In the crystal of Galβ$NHSO_2CH_2Cl$ (**31**), there is no direct hydrogen bonding between N1 and O1′. A finite

Table 7. Finite and infinite chain of hydrogen bonding in compounds **17**–**19**, **22**, **23**, **31**, and **32**.

Compound	Finite chain of hydrogen bonding	Infinite chain of hydrogen bonding
GlcβNHSO$_2$CH$_3$ (**17**)	N1−H1N···O4−H4O···O2−H2O···O6−H6O···O3−H3O···O2′	no infinite chain
GalβNHSO$_2$CH$_3$·H$_2$O (**18**)	N1−H1N···O3−H3O···O1W−H1W···O6−H6O···O2−H2O··· ···O4−H4O···O2′ O1W−H2W···O1′	no infinite chain
GlcNAcβNHSO$_2$CH$_3$·H$_2$O (**19**)	N1−H1N···O1′ N2−H2N···O1″	···O3−H3O···O6−H6O ···O1W−H2W···O3··· ···O4−H4O···O1W−H1W···O4···
CellβNHSO$_2$CH$_3$ (**22**)	N1A−H1NA···O2A−H2OA···O2D−H2OD···O6A−H6OA···O3C−H3OA···O5D O2C−H2OC···O4D−H4OD···O6B−H6OB···O4B−H4OB···O1′A N1C−H1NC···O3B, O3D−H3OD···O1′A O6C−H6OC···O1′C, O6D−H6OD···O6C	no infinite chain
LacβNHSO$_2$CH$_3$·H$_2$O (**23**)	N1−H1N···O1′ O4B−H4OB···O1W−H2W···O6A−H6OA···O2A−H2OA··· ···O2B−H2OB···O3A−H3OA···O5B O3A−H3OA···O6B, O1W−H1W···O2′	···O3B−H3OB···O6B−H6OB···O3B···
GalβNHSO$_2$CH$_2$Cl (**31**)	N1−H1N···O3−H3O···O2−H2O···O1′, O2−H2O···O2′, O4−H4O···O1′	O6−H6O···O6
GlcNAcβNHSO$_2$CH$_2$Cl·H$_2$O (**32**)	N1−H1N···O1′ N2−H2N···O1″	···O3−H3O···O6−H6O···O1W−H2W···O3··· ···O4−H4O···O1W−H1W···O4···

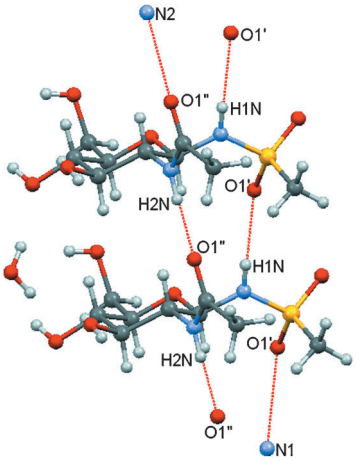

Figure 6. Representation of the double-pillared packing in GlcNAcβNHSO$_2$CH$_3$·H$_2$O (**19**).

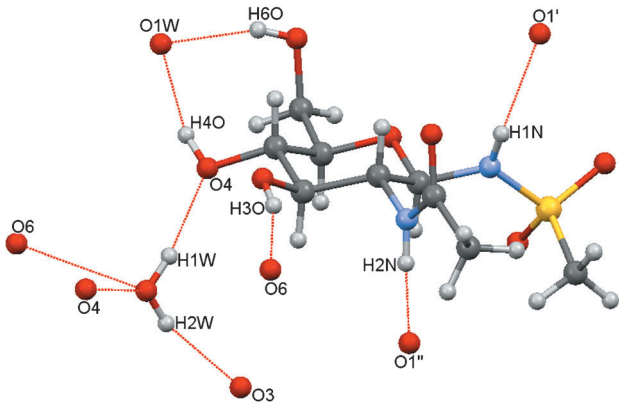

Figure 7. Finite and infinite chains of hydrogen bonds in GlcNAcβNHSO$_2$CH$_3$·H$_2$O (**19**).

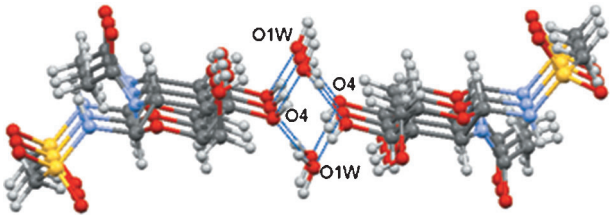

Figure 8. Formation of the homodromic cycle in GlcNAcβNHSO$_2$CH$_3$·H$_2$O (**19**).

chain starts from N1, passes through O3 and O2 of symmetry-related molecules and ends at O1′. The infinite chain involves O6 as a donor as well as acceptor (see Figure S4 in the Supporting Information). A direct hydrogen bond between O2−H and O2′ of another molecule is also present. O2−H2O acts as a bifurcated hydrogen donor for O1′ and O2′, whereas O1′ acts as a double acceptor for O2 and O4 atoms (O2−H2O···O1′···H4O−O4). The molecular packing of GlcNAcβNHSO$_2$CH$_2$Cl (**32**) is similar to that in GlcNAcβNHSO$_2$CH$_3$ (**19**) and the model GlcNAcβNHAc. N1 and O1′ and N2 and O1″ are connected through a finite chain of hydrogen bonds. The water molecule is tetra-coordinated, acting as donor for O3 and O4 and an acceptor for the atoms O4 and O6. The O6 atom also serves as an acceptor for O3−H3O.

C−H···X interactions: C−H···X (X = O/N/Cl) contacts were determined by using three geometrical parameters namely, the distance C···X representing the donor–acceptor distance (D–A); the distance H···X (H–A), the hydrogen bond length; and the C−H···X angle (θ). Only those interactions for which the D–A values are shorter than 3.6 Å and the θ values are greater than 110° are considered as significant (see Table 8). In GlcβNHSO$_2$CH$_3$ (**17**), two methyl hydrogens of the aglycon chain are involved in the C−H···O inter-

Table 8. C–H···O hydrogen bond parameters for compounds **17**–**19**, **22**, **23**, **31**, and **32**.

D–H···A	D–H [Å]	H–A [Å]	D–A [Å]	D–H···A [°]	Symmetry
$Glc\beta NHSO_2CH_3$ (**17**)					
C2′–H2′B···O1′	0.96	2.57	3.190	122.4	$-x, 1/2+y, 2-z$
C2′–H2′A···O2	0.96	2.65	3.492	147.3	$x, y, 1+z$
C3–H3···O2′	0.98	2.66	3.567	154.6	$1+x, y, z$
$Gal\beta NHSO_2CH_3{\cdot}H_2O$ (**18**)					
C2–H2···O5	0.98	2.70	3.424	131.1	$1.5-x, 1/2+y, -z$
C5–H5···O1′	0.98	2.71	3.619	154.8	$2-x, y, -z$
C6–H6B···O3	0.97	2.72	3.327	121.4	$x, -1+y, z$
$GlcNAc\beta NHSO_2CH_3{\cdot}H_2O$ (**19**)					
C2′–H2′A···O1″	0.96	2.62	3.537	159.2	$-1+x, y, z$
C2′–H2′B···O2′	0.96	2.40	3.340	166.8	$2-x, 1/2+y, 1-z$
C2′–H2′C···O2′	0.96	2.62	3.294	127.9	$1-x, 1/2+y, 1-z$
C1–H1···O1″	0.98	2.53	3.263	131.3	$-1+x, y, z$
C2″–H″B···O5	0.96	2.55	3.307	136.1	$x, 1+y, z$
C2″–H″C···O1′	0.96	2.61	3.403	139.9	$1+x, 1+y, z$
$Cell\beta NHSO_2CH_3$ (**22**)					
Molecule A (**22A**)					
C2′A–H′AA···O6C	0.96	2.59	3.118	114.9	$x, 1+y, 1+z$
C5A–H5A···O5D	0.98	2.54	3.434	152.5	$x, y, 1+z$
C1B–H1B···O3D	0.98	2.60	3.500	152.8	$x, 1+y, 1+z$
C5B–H5B···O3D	0.98	2.66	3.556	151.3	$x, 1+y, 1+z$
Molecule B (**22B**)					
C2′C–H′BC···O4D	0.96	2.34	3.254	159.6	$x, y, 1+z$
C1C–H1C···O2′A	0.98	2.49	3.414	156.7	$x, y, -1+z$
C5C–H5C···O2′A	0.98	2.56	3.469	154.4	$x, y, -1+z$
C2C–H2C···O2B	0.98	2.47	3.285	140.9	$2-x, -1/2+y, 1-z$
C6D–H6D2···O2B	0.97	2.70	3.409	130.4	$x, y, -1+z$
C6D–H6D2···O4A	0.97	2.55	3.497	164.4	$x, y, -1+z$
C5D–H5D···O2C	0.98	2.56	3.207	123.1	$2-x, -1/2+y, -z$
C3D–H3D···O6A	0.98	2.37	3.129	134.2	$x, -1+y, -1+z$
C6C–H6C2···O2A	0.97	2.66	3.563	155.8	$1-x, -1/2+y, 1-z$
$Lac\beta NHSO_2CH_3{\cdot}H_2O$ (**23**)					
C2′–H2′B···O3B	0.96	2.43	3.251	144.0	$2-x, 1/2+y, 1-z$
C2′-H2′A···O1W	0.96	2.64	3.257	122.4	$2-x, 1/2+y, 1-z$
C2′–H2′C···O1W	0.96	2.64	3.365	132.6	$1-x, 1/2+y, 1-z$
C5A–H5A···O6A	0.98	2.44	3.277	142.8	$-1+x, y, z$
C6A–H6A2···O2A	0.97	2.68	3.443	135.5	$x, y, 1+z$
C6B–H6B1···O2′	0.97	2.67	3.575	155.6	$2-x, -1/2+y, -z$
C3B–H3B···O4B	0.98	2.59	3.342	133.5	$1+x, y, z$
$Gal\beta NHSO_2CH_2Cl$ (**31**)					
C2′–H2′B···O2′	0.97	2.30	3.151	145.5	$-1+x, y, z$
C2–H2···O1′	0.98	2.66	3.198	114.9	$-x, 1/2+y, 1/2-z$
C3–H3···O4	0.98	2.51	3.353	143.8	$1+x, y, z$
$GlcNAc\beta NHSO_2CH_2Cl{\cdot}H_2O$ (**32**)					
C2′–H2′A···O2′	0.97	2.38	3.237	146.5	$-1/2+x, 1/2-y, -z$
C2″–H″B···O5	0.96	2.42	3.294	152.1	$x, -1+y, z$
C1–H1···O1″	0.98	2.44	3.181	132.1	$-1+x, y, z$
C3–H3···O1″	0.98	2.61	3.324	130.0	$-1+x, y, z$

actions (C2′–H2′B···O1′ and C2′–H2′A···O2). O2 and O2′ act as double acceptors (C2′–H2′A···O2···H4O–O4 and C3–H3···O2′···H3O–O3). There are only three C–H···O interactions (C2–H2···O5, C5–H5···O1′ and C6–H6B···O3) in $Gal\beta NHSO_2CH_3$ (**18**). As O1′ and O3 atoms are already accepting heteroatom-held (O/N) hydrogens, these serve as double acceptors. Examination of the C–H···O interactions in the crystal structure of $GlcNAc\beta NHSO_2CH_3$ (**19**) reveals the presence of a trifurcated hydrogen-bond pattern involving C1–H1···O1″···H2N–N2 and C2′–H2′A···O1″ (Figure 9). This trifurcated hydrogen bonding along with the direct hydrogen bond between N1 and O1′ may be the cause of the different aglycon conformation of $GlcNAc\beta NHSO_2CH_3$ (**19**) as compared to other methanesulfonamido derivatives. All three methyl hydrogens of the aglycon chain are involved in the C–H···O interactions (C2′–H2′B···O2′, C2′–H2′C···O2′ and C2′-H2′A···O1″) (Figure 9), which may also contribute to the altered aglycon conformation. O1′ and O2′ act as double acceptors. The molecular packing is also stabilized by one bifurcated hydrogen bond (N1–H1N···O1′···H″C–C2″) and one C–H···O interaction (C2″–H″B···O5) (Table 8).

The molecular packing of $Cell\beta NHSO_2CH_3$ (**22**) is stabilized by various C–H···O interactions leading to several bifurcated hydrogen bonds. O2A, O4D, O6A, O3D, O2′A, O6C, O5D, and O2B act as double acceptor atoms (N1A–H1NA···O2A···H6C2–C6C, O2C–H2OC···O4D···H′BC–C2′C, O2D–H2OD···O6A···H3D–C3D, C1B–H1B···O3D···H5B–C5B, C1C–H1C···O2′A···H5C–C5C, O6D–H6OD···O6C···H′AA–C2′A, C5A–H5A···O5D···H3OC–O3C and C2C–H2C···O2B ···H6D2–C6D). In addition to bifurcated hydrogen bonds, two C–H···O interactions are also seen (C6D–H6D2···O4A and C5D–H5D···O2C). The molecular packing of $Lac\beta NHSO_2CH_3$ (**23**) is also stabilized by various bifurcated hydrogen bonds involving O1W, O3B, O2A, O6A and O2′ atoms as double acceptors (C2′–H2′A···O1W···H2′C–C2′, C2′–H2′B···O3B···H6OB–O6B, C6A–H6A2···O2A···H6OA–O6A, C5A–H5A···O6A···H2W–O1W and C6B–H6B1···O2′···H1W–O1W). The molecular packing is further stabilized by one more C–H···O interaction (C3B–H3B···O4B) (Table 8).

In $Gal\beta NHSO_2CH_2Cl$ (**31**), the molecular packing is mainly stabilized by one trifurcated and one bifurcated hydrogen bond, where O1′ acts as a triple acceptor and O2 as a double acceptor (O2–H2O···O1′···H4O–O4 and C2–H2···O1′, O2–H2O···O2′···H2′B–C2′). One more C–H···O interaction (C3–H3···O4) is also noted. Examination of the C–H···O/N interactions in the crystal structure of

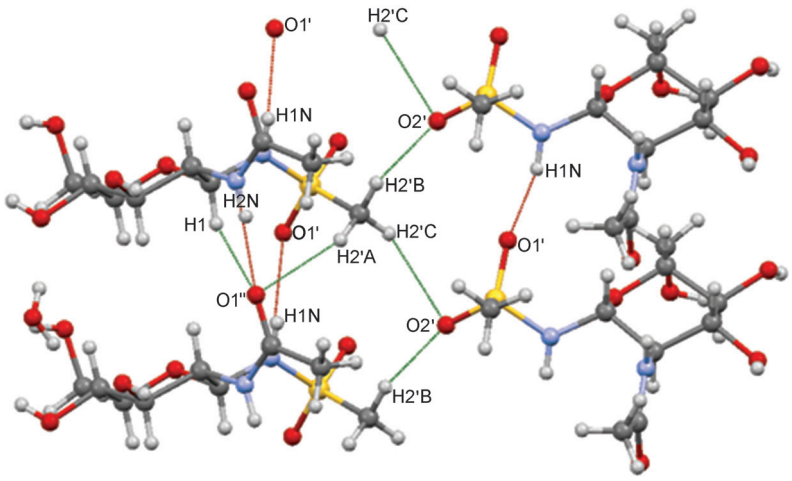

Figure 9. Presence of trifurcated hydrogen bonds and C–H···O interactions (green) of the aglycon chain in $GlcNAc\beta NHSO_2CH_3 \cdot H_2O$ (**19**).

$GlcNAc\beta NHSO_2CH_2Cl$ (**32**) reveals the presence of a trifurcated hydrogen bond pattern involving C1–H1···O1″···H2N–N2 and C3–H3···O1″ (Figure 10). This pattern is different from that of $GlcNAc\beta NHSO_2CH_3$ (**19**), as the third donor hydrogen in this case comes from C3–H rather than from C2′–H as in the case of compound **19** (C1–H1···O1″···H2N–N2 and C2′–H2′A···O1″). Only one hydrogen atom of the aglycon chain is involved in the C–H···O interaction (C2′–H2′A···O2′) leading to the formation of a helical assembly (Figure 11). Like $GlcNAc\beta NHSO_2CH_3$ (**19**), $GlcNAc\beta NHSO_2CH_2Cl$ (**32**) also shows a different aglycon conformation than $Gal\beta NHSO_2CH_2Cl$ (**31**), which may be due to the direct hydrogen bonding between N1···O1′ and the C–H···O interaction of the aglycon chain. The molecular packing is further stabilized by one C–H···O hydrogen bond formed by the methyl carbon of the C-2 acetamido moiety (C2″–H″B···O5). No C–H···N interaction is noted in any of the seven compounds studied. The chloromethanesulfonamido derivatives **31** and **32** did not display any C–H···Cl hydrogen bond in the crystal.

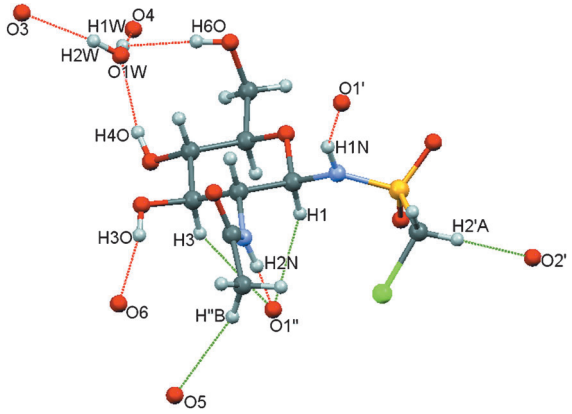

Figure 10. Presence of trifurcated hydrogen bonds, N–H···O and O–H···O (red) and C–H···O (green) interactions in $GlcNAc\beta NHSO_2CH_2Cl \cdot 1H_2O$ (**32**).

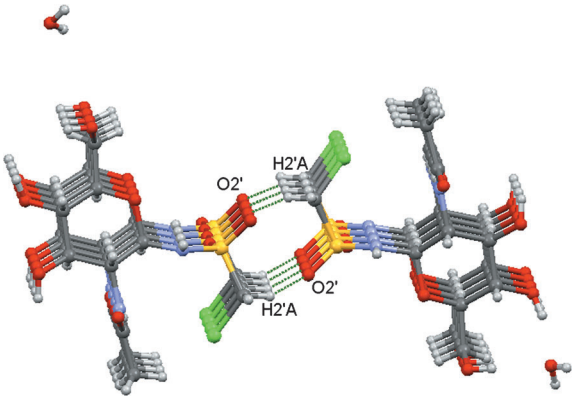

Figure 11. Presence of the hydrogen-bonded helical network (green) of the aglycon moiety in $GlcNAc\beta NHSO_2CH_2Cl \cdot 1H_2O$ (**32**).

Conclusion

A series of novel glycosyl sulfonamides have been designed as analogues of the *N*-glycoprotein linkage region and synthesized successfully in moderate to good yields. An improved procedure was developed for the preparation of *N*-(β-D-glycosyl)methanesulfonamides (**17**–**24**) from the corresponding glycosyl azides. A series of *N*-(β-D-glycopyranosyl) chloromethanesulfonamides (**30**–**34**) were also designed and synthesized as analogues of the *N*-glycoprotein linkage region. These compounds may have potential as glycogen phosphorylase inhibitors. Among all the compounds synthesized (**17**–**24** and **30**–**34**), crystal structures of seven of them have been solved as part of the present work. The influence of the structural variation of the glycan as well as the aglycon part on the key torsion angles (ω, ϕ_0, ψ_0, ϕ_N, ψ_N, and χ_2) was examined. A comparative analysis of the ϕ_N values showed that the torsion angle ϕ_N does not alter significantly by changing the carboxamido group to the sulfonamido moiety as compared to that of the model compound GlcNAcβNHAc. For most of the compounds (**17**, **18**, **22**, **23**, and **31**), the value of the torsion angle ψ_N was close to 75° except for methanesulfonamido (**19**) and chloromethanesulfonamido (**32**) derivatives of GlcNAc. Lastly, the side chain torsion angle χ_2 of $Gal\beta NHSO_2CH_2Cl$ (**31**) and $GlcNAc\beta NHSO_2CH_2Cl$ (**32**) differ substantially, resulting in a turnaround of the conformation about S1–C2′ from close to *anti* in **31** to *syn* in **32**. This large variance may be due to differences in the molecular packing.

A comprehensive analysis of the molecular packing stabilized by hydrogen bonds and C–H···O interactions in the crystal structures of all the sulfonamides was also carried out. The molecular packing of GlcNAcβNHSO$_2$CH$_3$ (**19**), LacβNHSO$_2$CH$_3$ (**23**), GalβNHSO$_2$CH$_2$Cl (**31**), and GlcNAcβNHSO$_2$CH$_2$Cl (**32**) is stabilized by finite as well as infinite chains of hydrogen bonds. Bioisosteric replacement of the carboxamide with sulfonamide causes a few changes in the molecular packing. The most significant of these changes is the absence of a C2′–H2′···O1′ interaction in the sulfonamido derivatives **19** and **32**. This characteristic C–H···O interaction plays an important role in the formation of the anti-parallel bifurcated double-pillared hydrogen bond network, a hallmark feature of the molecular packing of the models (GlcNAcβNHAc and GlcNAcβAsn) of the conserved *N*-glycoprotein linkage region. In both these compounds (**19** and **32**), C2′ of the aglycon chain is involved in the interaction with the other sulfonamido oxygen atom, namely, O2′ (C2′–H2′···O2′). The characteristic feature of the molecular packing of GlcNAcβNHSO$_2$CH$_3$ (**19**) and GlcNAcβNHSO$_2$CH$_2$Cl (**32**) is the presence of a trifurcated hydrogen bond involving O1″ as a triple acceptor atom, which was also seen in the case of GlcNAcβNHAc. The direct hydrogen bonding between N1 and O1′ seems to be a distinctive molecular recognition motif that controls the aglycon conformation in compounds **19** and **32**. Besides this, the weaker C–H···O contacts also play a co-operative role in controlling the conformation of the aglycon moiety. The above structural analysis shows that glycosyl sulfonamides due to insignificant deviation in the ϕ_N value may serve as linkage region analogues. This study illustrated for the first time the effect of the bioisosteric replacement of a carboxamide group by a sulfonamide group on the *N*-glycosidic torsion ϕ_N as well as on the molecular assembly.

Table 9. Data collection and refinement statistics for compounds **17**–**19**, **22**, **23**, **31**, and **32**.

Parameter	**17**	**18**	**19**	**22**	**23**	**31**	**32**
empirical formula	$C_7H_{15}N\ O_7S$	$C_7H_{17}NO_8S$	$C_9H_{20}N_2O_8S$	$C_{13}H_{25}NO_{12}S$	$C_{13}H_{27}O_{13}S$	$C_7H_{14}ClNO_7S$	$C_9H_{19}ClN_2O_8S$
formula weight	257.26	275.28	316.33	419.40	437.42	291.70	350.77
temp [K]	298(2)	298 (2)	297(2)	293(2)	298(2)	293(2)	298(2)
λ [Å]	0.71073	0.71073	0.71073	0.71073	0.71073	0.71073	0.71073
crystal system	monoclinic	monoclinic	monoclinic	monoclinic	monoclinic	orthorhombic	orthorhombic
space group	$P2_1$	$C2$	$P2_1$	$P2_1$	$P2_1$	$P2_12_12_1$	$P2_12_12_1$
a [Å]	6.8460(3)	19.1916(15)	4.9905(2)	12.8879(2)	4.8289(2)	4.9221(2)	5.0424(6)
b	9.7882(4)	7.5767(5)	7.8973(2)	10.0481(2)	26.0236(8)	9.6824(5)	7.8402(10)
c [Å]	8.6000(4)	9.4859(8)	18.6950(7)	14.6387(4)	7.5513(2)	24.2790(11)	38.401(5)
α [°]	90	90	90	90	90	90	90
β [°]	107.059(2)	117.126(4)	96.455(2)	107.7850(10)	101.805(2)	90	90
γ [°]	90	90	90	90	90	90	90
volume [Å^3]	550.93(4)	1227.62(16)	732.13(4)	1805.10(7)	928.87(5)	1157.08(9)	1518.1(3)
Z	2	4	2	4	2	4	4
ρ_{calcd} [Mg m^{-3}]	1.551	1.489	1.435	1.543	1.564	1.674	1.535
μ [mm^{-1}]	0.315	0.294	0.259	0.245	0.246	0.535	0.428
F(000)	272	584	336	888	464	608	736
crystal size [mm]	0.55×0.25×0.20	0.38×0.25×0.22	0.38×0.22×0.18	0.35×0.22×0.18	0.32×0.28×0.20	0.30×0.20×0.20	0.38×0.25×0.22
theta range [°]	2.48 to 25.00	2.94 to 24.97	3.39 to 25.00	2.50 to 25.00	2.76 to 25.00	2.26 to 25.00	2.65 to 24.99
index ranges	$-8h\le7$, $-11\le k\le10$, $-10\le l\le10$	$-22\le h\le22$, $-8\le k\le8$, $-11\le l\le8$	$-5\le h\le5$, $-9\le k\le6$, $-18\le l\le22$	$-13\le h\le15$, $-11\le k\le11$, $-17\le l\le17$	$-5\le h\le4$, $-30\le k\le30$, $-8\le l\le8$	$-5\le h\le3$, $-11\le k\le10$, $-28\le l\le28$	$-5\le h\le5$, $-9\le k\le7$, $-45\le l\le31$
reflections collected/ unique	3438/1594 [R(int) = 0.0199]	3716/2074 [R(int) = 0.0135]	4498/2381 [R(int) = 0.0195]	11245/6030 [R(int) = 0.0214]	5795/3014 [R(int) = 0.0172]	6048/1961 [R(int) = 0.0164]	6162/2626 [R(int) = 0.0225]
completeness to theta [%]	97.0	98.9	99.7	99.9	94.7	98.0	99.8
refinement method	full-matrix least-squares on F^2	full-matrix least-squares on F^2	full-matrix least-squares on F^2	full-matrix least-squares on F^2	full-matrix least-squares on F^2	full-matrix least-squares on F^2	full-matrix least-squares on F^2
data restraint parameters	1594/1/154	2074/4/172	2381/4/194	6030/3/526	3014/5/273	1961/1/162	2626/5/207
goodness-of fit on F^2	1.082	1.094	1.048	1.027	1.092	1.061	1.071
final R indices [$I>2\sigma(I)$]	$R1$ = 0.0277, $wR2$ = 0.0706	$R1$ = 0.0212, $wR2$ = 0.0558	$R1$ = 0.0282, $wR2$ = 0.0726	$R1$ = 0.0317, $wR2$ = 0.0731	$R1$ = 0.0281, $wR2$ = 0.0675	$R1$ = 0.0259, $wR2$ = 0.0652	$R1$ = 0.0501, $wR2$ = 0.1209
R indices (all data)	$R1$ = 0.0285, $wR2$ = 0.0712	$R1$ = 0.0224, $wR2$ = 0.0573	$R1$ = 0.0292, $wR2$ = 0.0732	$R1$ = 0.0361, $wR2$ = 0.0757	$R1$ = 0.0301, $wR2$ = 0.0687	$R1$ = 0.0270, $wR2$ = 0.0661	$R1$ = 0.0555, $wR2$ = 0.1245

Experimental Section

Preparation of single crystals and X-ray crystallographic analysis: Single crystals of the compounds **17**–**19**, **22**, **23**, **31**, and **32** were obtained from aqueous methanol by slow evaporation at room temperature. X-ray data collection was performed by using a Bruker AXS Kappa Apex II CCD diffractometer equipped with graphite-monochromated Mo (Kα) (λ = 0.7107 Å) radiation. A crystal fixed at the tip of the glass fiber was mounted on the goniometer head with the aid of a video microscope. The automatic cell determination routine, with 36 frames at three different orientations of the detector was employed to collect reflections for unit cell determination. Thereafter, intensity data for the structure determination were collected through an optimized strategy which gave an average fourfold redundancy. The program APEX2-SAINT[26] was used for integrating the frames. The fourfold redundancy per reflection was utilized for achieving good multi-scan absorption correction using the program SADABS.[27] Besides absorption, Lorentz, polarization, and decay corrections were applied during data reduction. The structures were solved by direct methods using SIR92[28] and refined by full-matrix least squares techniques using the SHELXL-97[29] computer program.

All hydrogen atoms attached to carbon were fixed at chemically meaningful positions and a riding model refinement was applied. The nitrogen hydrogen atoms were located by using a difference Fourier map and refined with isotropic thermal parameters. All the hydrogen atoms of the hydroxyl groups could be located in the difference Fourier map. The free refinement of these hydrogens did not yield satisfactory O−H distances in all the cases. Hence, these atoms were fixed at geometrically meaningful positions and were allowed to ride over the respective oxygen atoms during the refinement. The starting coordinates of the hydrogen atoms were chosen from Fourier peak positions. The thermal parameters of these hydrogen atoms were fixed at 1.5 times the equivalent thermal parameters of the parent oxygen. The O−H distances were judiciously fixed after the inspection of distances in the difference map. The details of the O−H hydrogen fixing in individual structures are described in the respective cif files. The water hydrogen atoms were located in the difference Fourier map and refined with O−H distances restrained to 0.82 Å. The H-O-H angles were also restrained to near tetrahedral values. Molecular graphics were drawn using ORTEP32[30] and Mercury programs.[31] The relevant details for the data collection and refinement are given in Table 9.

CCDC-932532 (**17**), CCDC-932533 (**18**), CCDC-932534 (**19**), CCDC-932535 (**22**), CCDC-932536 (**23**), CCDC-932537 (**31**), and CCDC-932538 (**32**) contain the supplementary crystallographic data for this paper. These data can be obtained free of charge from The Cambridge Crystallographic Data Centre via www.ccdc.cam.ac.uk/data_request/cif.

Acknowledgements

This work was supported by Indo-French Centre for Promotion of Advanced Research (IFCPAR), New Delhi. The funding provided by the Department of Science and Technology, New Delhi, for the purchase of a 400 MHz NMR under IRHPA Scheme and ESI-MS under the FIST program is gratefully acknowledged. The authors thank the single crystal X-ray facility, Chemistry Department, IIT Madras for the X-ray data collection. We are thankful to Mr. V. Ram Kumar for X-ray data collection and cooperation. One of us (A.S.) is thankful to the Council of Scientific and Industrial Research (CSIR), New Delhi, for the award of a Senior Research Fellowship. We also thank Cambridge Crystallographic Data Centre (CCDC), UK, for making the program Mercury 3.1 available for use.

[1] A. Varki, R. D. Cumming, J. D. Esko, H. H. Freeze, P. Stanley, C. R. Bertozzi, G. W. Hart, M. E. Etzler, *Essential of Glycobiology*, 2nd ed, Cold Spring Harbor Laboratory, **2009**.
[2] A. Varki, *Glycobiology* **1993**, *3*, 97–130.
[3] R. A. Dwek, *Chem. Rev.* **1996**, *96*, 683–720.
[4] T. Lakshmanan, D. Sriram, K. Priya, D. Loganathan, *Biochem. Biophys. Res. Commun.* **2003**, *312*, 405–413.
[5] D. Loganathan, U. Aich, T. Lakshmanan, *Proc. Indian Natl. Sci. Acad.* **2005**, *71*, 213–235.
[6] D. Loganathan, U. Aich, *Glycobiology* **2005**, *16*, 343–348.
[7] M. M. N. Ali, U. Aich, B. Varghese, S. Pérez, A. Imberty, D. Loganathan, *J. Am. Chem. Soc.* **2008**, *130*, 8317–8325.
[8] M. M. N. Ali, U. Aich, S. Pérez, A. Imberty, D. Loganathan, *Carbohydr. Res.* **2009**, *344*, 355–361.
[9] G. Cioci, A. Srivastava, D. Loganathan, S. A. Mason, S. Pérez, A. Imberty, *J. Am. Chem. Soc.* **2011**, *133*, 10042–10045.
[10] M. Mathiselvam, B. Varghese, D. Loganathan, *Glycoconjugate J.* **2011**, *28*, 573–580.
[11] A. Srivastava, B. Varghese, D. Loganathan, *J. Carbohydr. Chem.* **2012**, *31*, 31–47.
[12] P. A. Colinas, R. D. Bravo, *Carbohydr. Res.* **2007**, *342*, 2297–2302.
[13] P. A. Colinas, R. D. Bravo, *Org. Lett.* **2003**, *5*, 4509–4511.
[14] T. Y. Shen, J. P. Li, C. P. Dorn, D. Ebel, R. Bugianesi, R. Fecher, *Carbohydr. Res.* **1972**, *23*, 87–102.
[15] A. P. Butera, J. D. S. Filho, D. T. Carvalho, R. C. Figueiredo, L. C. A. Faria, M. A. Nunes, M. A. F. Prado, R. J. Alves, M. H. Andrade, A. T. Silva, *Quim. Nova* **2007**, *30*, 1267–1274.
[16] P. A. Colinas, C. A. Témpera, O. M. Rodríguez, R. D. Bravo, *Synthesis* **2009**, *24*, 4143–4148.
[17] Z. Gyorgydeak, J. Theim, *Adv. Carbohydr. Chem. Biochem.* **2005**, *60*, 103–182.
[18] R. Ghosh, A. Chakraborty, S. Maiti, *Tetrahedron Lett.* **2004**, *45*, 9631–9634.
[19] F. M. Ibatullin, K. A. Shabalin, *Synth. Commun.* **2000**, *30*, 2819–2823.
[20] G. A. Jeffrey, *Acta Crystallogr. Sect. B* **1990**, *46*, 89–103.
[21] J. Ohanessian, D. Avenel, A. Neuman, H. Gillier-Pandraud, *Carbohydr. Res.* **1980**, *80*, 1–13.
[22] A. D. French, *Adv. Carbohydr. Chem. Biochem.* **2012**, *67*, 19–92.
[23] Z. Peralta-Inga, G. P. Johnson, M. K. Dowd, A. J. Rendleman, E. D. Stevens, A. D. French, *Carbohydr. Res.* **2002**, *337*, 851–861.
[24] T. Lakshmanan, D. Sriram, D. Loganathan, *Acta Crystallogr. Sect C: Struct. Commun.* **2001**, *57*, 825–826.
[25] A. Parkin, A. Collins, C. J. Gilmore, C. C. Wilson, *Acta Crystallogr.-Sect. B* **2008**, *64*, 66–71.
[26] Bruker, APEX2, SAINT-Plus and XPREP, Bruker Axs Inc., Madison, Wisconsin, USA, **2004**.
[27] Bruker SADABS, Bruker AXS Inc., Madison, Wisconsin, USA, **1999**.
[28] A. Atarmare, G. Gascarano, C. Giacovazzo, A. Guagliardi, *J. Appl. Crystallogr.* **1993**, *26*, 343–350.
[29] G. M. Sheldrick, SHELXL97, Program for Crystal Structure Refinement; University of Göttingen, Göttingen (Germany), **1997**.
[30] ORTEP-3 for Windows-a version of ORTEP-III with a Graphical User Interface (GUI): L. J. Farrugia, *J. Appl. Crystallogr.* **1997**, *30*, 565.
[31] I. J. Bruno, J. C. Cole, P. R. Edgington, M. Kessler, C. F. Macrae, P. McCabe, J. Pearson, R. Taylor, *Acta Crystallogr.Sect. B* **2002**, *58*, 389–397.
[32] D. Sriram, T. Lakshmanan, D. Loganathan, S. Srinivasan, *Carbohydr. Res.* **1998**, *309*, 227–236.
[33] D. Sriram, H. Sreenivasan, S. Srinivasan, K. Priya, M. Vishnu Thirtha, D. Loganathan, *Acta Crystallogr.Sect. C* **1997**, *53*, 1075–1077.
[34] U. Aich, T. Lakshmanan, B. Varghese, D. Loganathan, *J. Carbohydr. Chem.* **2003**, *22*, 883–893.

Please note: Minor changes have been made to this manuscript since its publication in *Chemistry – A European Journal* Early View. The Editor.

Received: May 25, 2013

